Palaeogeography, Palaeoclimatology, Palaeoecology 397 (2014) 31–37

Contents lists available at ScienceDirect

Palaeogeography, Palaeoclimatology, Palaeoecology

journal homepage: www.elsevier.com/locate/palaeo

Change in the intensity of low-salinity water inflow from the Bay of Bengal into the Eastern Arabian Sea from the Last Glacial Maximum to the Holocene: Implications for monsoon variations

B.S. Mahesh [1], V.K. Banakar *

CSIR-National Institute of Oceanography, Dona Paula, Goa 403 004, India

ARTICLE INFO

Article history:
Received 27 March 2012
Received in revised form 15 May 2013
Accepted 20 May 2013
Available online 28 May 2013

Keywords:
Arabian Sea
Indian monsoon
Paleo-Sea Surface Temperature
Paleo-salinity
Planktonic foraminifera $\delta^{18}O$ and Mg/Ca

ABSTRACT

A 100–400 km wide region of the coastal Eastern Arabian Sea (EAS), off the west-coast of India, is characterized by a low-salinity tongue formed by the inflow of low-salinity surface water from the Bay of Bengal (BoB). This low-salinity tongue is largely driven by the sea level higher in BoB than in the Arabian Sea and by alongshore pressure gradient between southern- and northern-EAS, and is expected to respond to summer monsoon freshwater flux to the bay. Here, we report past variation in the relative intensity of summer- and winter-monsoons based on changes in the north–south salinity gradient within this low-salinity tongue. The salinity gradient is estimated from paired measurement of $\delta^{18}O$ and Mg/Ca in *Globigerinoides sacculifer* extracted from sediment cores collected at northern high-salinity and southern low-salinity locations within this tongue.

The Last Glacial Maximum (LGM) to peak-Holocene $\delta^{18}O$ and sea surface temperature gradients at both locations are ~ −2‰ and +2 °C respectively, while the sea surface salinity gradient at northern-EAS is 0.5 psu higher than in the southern-EAS, suggesting distinctly different SSS structure in the LGM-EAS. The north–south surface salinity gradient was also larger by ~0.5 psu during the LGM (1.2 psu) as compared to the gradient during the Holocene (0.7 psu). Increased north–south surface salinity gradient during the LGM suggests diminished flow of low-salinity water into the coastal EAS caused by combined effect of decreased freshening of the BoB and reduced seasonal mountain-river discharge into the EAS. Such surface hydrographic conditions in the coastal EAS clearly indicate significantly weakened summer monsoons and strengthened winter monsoons during the LGM.

1. Introduction

The sea surface-temperature (SST) and -salinity (SSS) in the Eastern Arabian Sea (EAS) are readily influenced by the strength of seasonally reversing monsoons, characteristic of the northern Indian Ocean. The monsoon dynamics also drive the inter-basin exchange of surface water between perennially less-saline Bay of Bengal (BoB) and more-saline Arabian Sea (Shetye et al., 1991; Shankar and Shetye, 2001). Evaporation dominant ($E–P > 1$) conditions in the Arabian Sea, and precipitation dominant ($E–P < 1$) conditions in the BoB, together result in distinctly different SSS structure between these two basins (Prasanna Kumar and Prasad, 1999; Wilson-Diaz et al., 2009). The contrasting E–P along with local wind forcing during the post-summer monsoon period cause differing sea levels between the southeast- and southwest-coasts of India, which result in alongshore pressure gradient, forcing the low-salinity BoB water to flow into the EAS (Shankar and Shetye, 2001). Model runs have been able to reproduce this climatological set-up, driving the low-salinity water plume entering into the EAS from BoB (Vinaychandran and Kurian, 2008). The local surface water $\delta^{18}O$ is sensitive to change SSS, and can be extracted from the isotopic signal of planktonic foraminifera when its SST component is estimated from Mg/Ca ratios. In modern conditions, the SST cooling associated with increased (decreased) SSS reflects relatively stronger winter (summer) monsoon.

A low salinity plume originating in the eastern coastal region of India (western BoB) during the post summer monsoons (i.e., Winter–Fall) travels around Sri Lanka, enters into southern-EAS and penetrates northward up to 15°N latitude (off Goa) as a low-salinity tongue (Fig. 1). This tongue is quite wide (~400 km) at the entry point (southern-EAS) and narrows as it travels northward. The cause of this low-salinity plume is attributed to the higher sea level in BoB than in the Arabian Sea and the prevailing wind system in the region (Shankar and Shetye, 2001). The BoB receives 50 times more freshwater (~100,000 m^3/s) than the EAS (~200 m^3/s) during the summer monsoon (University of Wisconsin—Madison, 2010). This in turn establishes alongshore density gradient and differing sea levels between the east (high) and west coast (low) of India resulting in intense poleward flowing plume of low salinity water into the EAS following the summer monsoons. As a consequence, ~6 Sv of low-salinity BoB water is advected into the EAS (Shankar,

---

* Corresponding author.
E-mail address: banakar@nio.org (V.K. Banakar).

[1] Present address: National Centre for Antarctic and Ocean Research, Headland Sada, Vasco-da-Gama, Goa, India.

http://dx.doi.org/10.1016/j.palaeo.2013.05.024

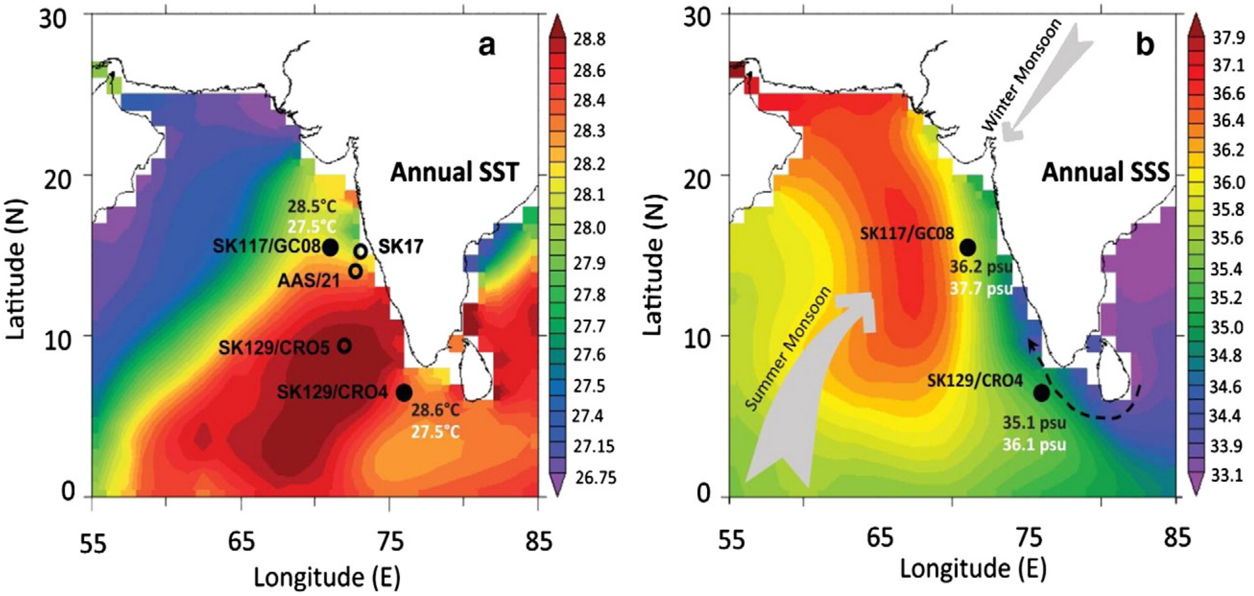

Fig. 1. Location of the studied sediment cores (filled circles) are shown on both annual surface temperature (a) and surface salinity (b) distribution maps (www.noaa.nodc.gov). The locations of the other published Mg/Ca-SST records are shown with open circles on SST map (a). Highly simplified trajectories of seasonally reversing monsoon winds are shown with shaded gray arrows on annual salinity map (b). The thickness of arrow indicates relative strength of modern summer (thick = strong) and winter (thin = weak) monsoons. Climate stage averaged surface salinity values at the studied core locations are shown with white fonts (Last Glacial Maximum) and black font (Holocene). The low-salinity water advection into the EAS from BoB is shown with a broken arrow.

2000), which is already preconditioned with lowered salinity due to summer monsoon overhead precipitation and seasonal outflow of medium to small rivers draining the Deccan Mountains. Hence, the EAS is distinctly marked with low-salinity water bounded to the north and west by high-salinity waters characteristic of the Arabian Sea (HSW). The SSS in this low-salinity tongue gradually increases from southern-EAS as it moves poleward and becomes indistinguishable at central-EAS (off Goa) due to overwhelming influence of HSW. Thus, the dynamics of this low-salinity plume in the EAS is dictated by the Indian monsoon system. Therefore, the temporal variation in the north–south SSS gradient in this low salinity tongue may be useful to understand the past changes in relative intensities of summer and winter monsoons. Keeping the river discharge and overhead precipitation driven freshening of the Arabian Sea and BoB as a basis, the relative increase in summer monsoons would strengthen the low-salinity tongue in the EAS; While, the relative weakening of summer monsoons would tend to reduce the SSS contrast between the two basins or weaken this tongue. This forms the preamble for the present study.

Here, we report the past changes in north–south SSS-gradient within the low-salinity tongue to understand variability of summer and winter monsoons since the Last Glacial Maximum (LGM). For this, two sediment cores collected at two ends of the low-salinity tongue are used. The northern core is located presently at the termination of low-salinity tongue where influence of HSW is distinctly evident by SSS of >36 psu and narrow low SSS band (<100 km wide). The southern core, on the other hand, is located at the entry of low-salinity tongue, which is evident by distinctly low-SSS water (<35 psu) and broad low-SSS band (>400 km wide) (Fig. 1). Paired measurements of $\delta^{18}O$ and Mg/Ca in *Globigerinoides sacculifer* (without terminal sac) were utilized to estimate SST and $\delta^{18}O_{SEAWATER}$ to reconstruct past changes in the SSS.

2. Materials and methods

The upper 150 cm section of two ~5 m long sediment cores from EAS (SK117/GC08 and SK129/CR04: Fig. 1) were used for the present study. The former core was collected at 15°29.67′N & 71°00.98′E (henceforth 'northern location') and the latter at 06°29.65′N & 75°58.68′E (henceforth 'southern location' for convenience). The water depths at these two locations are 2500 and 2000 m respectively. The sediment cores were sub-sampled at 2 cm intervals. The depth in sediment cores was translated into calendar ages based on eight (per sediment core) reservoir corrected (600 yr for the study region: http://calib.qub.ac.uk/marine/) AMS ^{14}C dates calibrated using on-line HULU calibration program (Danzeglocke et al., 2009) (Table 1), and estimated linear sedimentation rates between two dated sections (Fig. 2). The core-top age for northern location core is 2259 ± 64 yr BP and for southern core is 3048 ± 67 yr BP. The last dated sections correspond to 34,124 ± 402 and 32,564 ± 386 yr BP respectively. Thus complete LGM and most part of the Holocene period is retrieved.

The *Globigerinoides sacculifer* is a spinose mixed-layer dwelling planktic foraminifer (Hemleben et al., 1989) calcifying in a narrow depth range of 25–40 m (Farmer et al., 2007), which is relatively more resistant to dissolution compared to other planktic foraminifera (Delaney et al., 1985; Dekens et al., 2002), having nearly uniform

Table 1
Details of the sections dated by AMS-radiocarbon along with the laboratory references.

Sample code	Depth in core	Lab code		^{14}C measured age		Calendar age	
	(cm)	AA	LAB #	yr BP	±yr	Cal yr BP	±yr
SK117/GC08	1	1566	Utrecht	2847	26	2259	64
	15	AA79596	X10218A	7775	52	8000	37
	25	AA79597	X10219A	11,546	74	12,887	100
	49	AA79598	X10220	16,031	91	18,519	298
	79	AA79599	X10221	21,660	150	25,214	393
	103	AA79600	X10222A	25,910	230	30,180	230
	125	AA79601	X10223	30,140	450	33,805	433
	149	AA79602	X10224	30,550	460	34,124	402
SK129/CR04	1.5	AA79603	X10225	2533	38	1885	42
	20	AA79604	X10226	7144	53	7466	38
	40	AA79605	X10227	12,616	85	14,005	224
	48	AA79606	X10228	14,190	110	16,563	383
	70	AA79607	X10229	19,060	120	22,073	327
	80	AA79608	X10230	21,660	360	25,216	535
	100	AA79609	X10231	23,940	190	28,100	243
	120	AA79611	X10233	26,160	260	30,556	481
	150	AA79610	X10232	28,370	340	32,369	364